Magnetic and transport properties of $UCuP_2$ and $UCuAs_2$ pnictides

1991 J. Phys.: Condens. Matter 3 4959

(http://iopscience.iop.org/0953-8984/3/26/016)

J. Phys.: Condens. Matter 3 (1991) 4959–4970. Printed in the UK

Magnetic and transport properties of $UCuP_2$ and $UCuAs_2$ pnictides

D Kaczorowski†, R Troć† and H Noël‡

† W Trzebiatowski Institute for Low Temperature and Structure Research, Polish Academy of Sciences, PO Box 937, 50–950 Wrocław, Poland

‡ Laboratoire de Chimie Minérale B, CNRS, Université de Rennes, 35042 Rennes, France

Received 12 October 1990

Abstract. We have made detailed investigations of the magnetic and transport properties of the tetragonal compounds $UCuP_2$ and $UCuAs_2$ on single-crystal specimens. The present data indicate that both these compounds are ferromagnets below 75 K and 133 K with spontaneous magnetic moments of $0.98\mu_B$ and $1.27\mu_B$, respectively, and in the magnetically ordered region they exhibit high values of magnetocrystalline anisotropy constants. The electrical resistivity of $UCuP_2$ and $UCuAs_2$ at low temperatures behaves as T^2 while, in the temperature range above T_C, the observed negative slope of $\rho(T)$ may point to their Kondo lattice behaviour.

1. Introduction

In the course of our systematic search for new ternary uranium compounds occurring in the U–T–X systems (T is a transition metal and X is a pnictogen) up to now we have succeeded in identifying as many as six ternaries with the stoichiometry 1:1:2, namely $UCuP_2$, $UCuAs_2$, $UNiAs_2$, $UCoP_2$, $UPdAs_2$ and $UNiSb_2$ [1, 2]. All the above 1:1:2 pnictides, except for $UCuP_2$, crystallize in a tetragonal symmetry with $P4/nmm$ space group (the filled ZrSiS-type structure) [3–5]. $UCuP_2$ also has tetragonal symmetry and adopts the filled UGeTe-type structure (space group, $I4/mmm$) [6]. In contrast with the remaining ternaries which are antiferromagnets [2, 4, 5], $UCuP_2$ and $UCuAs_2$ order ferromagnetically at low temperatures [1, 2].

In the present paper we report the results of a detailed study on the magnetic and electrical transport properties of $UCuP_2$ and $UCuAs_2$, measured on single-crystal specimens.

2. Experimental details

Polycrystalline samples of $UCuP_2$ and $UCuAs_2$ were prepared by annealing stoichiometric mixtures of powdered copper metal and the appropriate uranium dipnictide (UP_2 or UAs_2) placed in vacuum-sealed quartz tubes and kept for 2 weeks at about 850 °C for the phosphide and 700 °C for the arsenide. Single crystals of these compounds were grown by the chemical vapour transport method using iodine as a transporting

0953-8984/91/264959 + 12 $03.50

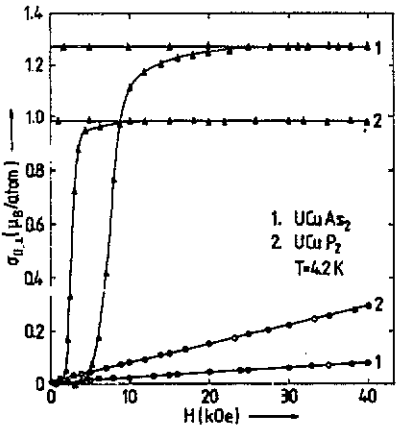

Figure 1. Magnetization versus magnetic field at 4.2 K of $UCuP_2$ and $UCuAs_2$ single crystals along (▲, △) and perpendicular (●, ○) to the *c* axis: ▲, ●, the magnetization data obtained in an increasing magnetic field; △, ○, magnetization data obtained in a decreasing magnetic field.

agent, as reported previously [3, 6]. The crystals obtained were in the form of thin plates perpendicular to the crystallographic *c* axis with maximum dimensions 10 mm × 10 mm × 0.2 mm.

Magnetic susceptibility measurements on the powder samples were performed in the temperature interval 4.2–1000 K using the Faraday method. The transverse magnetic susceptibility component $\chi_\perp$ and longitudinal magnetic susceptibility component $\chi_\parallel$ (both related to the *c* axis) were measured over the temperature range 4.2–300 K using a SQUID magnetometer at the University of Rennes.

Magnetization studies were carried out within the temperature interval 4.2–150 K and in applied magnetic fields up to 4 T by using a moving-sample magnetometer with a superconducting coil.

The electrical resistivities $\rho_\perp$ of $UCuP_2$ and $UCuAs_2$ were measured between 4.2 and 300 K, only in the basal plane, using a conventional four-point DC method. The current and voltage leads were attached to the samples by ultrasonic welding.

3. Results

3.1. Magnetization

Figure 1 displays the magnetizations $\sigma_\parallel$ and $\sigma_\perp$ measured at 4.2 K on single crystals of $UCuP_2$ and $UCuAs_2$ up to 4 T. Both investigated compounds were found to be strongly anisotropic with the easy-magnetization direction being along the *c* axis of the tetragonal unit cell. A straight-line behaviour $\sigma_\perp(H)$ and the absence of any hysteresis indicate that there is no transverse component of the spontaneous magnetic moment, i.e. the magnetic moments are strongly aligned along the *c* axis. The values of the ordered magnetic moment μ_s, measured with $H \parallel c$ are $0.98\mu_B$ per U atom and $1.27\mu_B$ per U atom for $UCuP_2$ and $UCuAs_2$, respectively. It appears that these values are considerably reduced in comparison with those expected for either the U^{4+} ($3.20\mu_B$) or U^{3+} ($3.27\mu_B$) free ions. This feature is mainly caused by splitting of the uranium ground multiplet

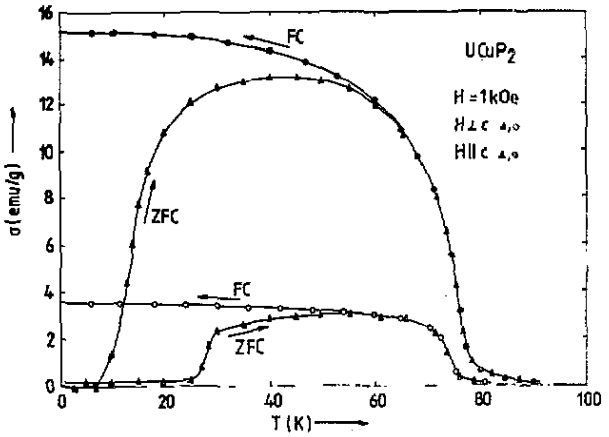

Figure 2. Magnetization versus temperature for a $UCuP_2$ single crystal in magnetic fields parallel and perpendicular to the c axis. The FC and ZFC curves were obtained by cooling the sample with and without an applied magnetic field, respectively. Note that 1 emu $g^{-1} \equiv 0.065\mu_B$.

under the crystal-field potential. Simultaneously, it seems reasonable to assume that the Kondo-like screening effect (as we shall see below, this effect was evidenced on the basis of electrical resistivity measurements) also plays an important role in the reduction in the resulting μ_s. As one can infer from figure 1, $UCuP_2$ and $UCuAs_2$ have rather high values of the nucleation field B_{nf} of magnetization which amount to 0.3 T and 0.5 T, respectively. These large values of B_{nf}, characteristic also for the UAsY (Y ≡ S, Se, Te) compounds [7, 8], can be explained by the assumption of a compensated narrow-wall domain structure which is reconstructed at B_{nf}.

On the basis of the data presented in figure 1, one can estimate the magnitude of the uniaxial anisotropy existing in $UCuP_2$ and $UCuAs_2$. The anisotropy energy in a tetragonal lattice may be expressed as follows:

$$E_a = K_1 \sin^2 \theta + K_2 \sin^4 \theta + \dots \tag{1}$$

where K_1 and K_2 are the anisotropy constants and θ denotes the angle of the magnetization vector with the c axis. In the case of the easy-magnetization direction along the c axis the constants K_1 and K_2 can be determined from the relation

$$H/\sigma_\perp = 2K_1/\sigma_s^2 + (2K_2/\sigma_s^4)\sigma_\perp \tag{2}$$

where σ_s is the spontaneous magnetization. The calculated values of K_1 for $UCuAs_2$ and $UCuP_2$ based on the above formula are about 5×10^6 J m^{-3} and 9×10^5 J m^{-3}, respectively. The calculated constant K_2 has been found to be negligible in both cases. The corresponding anisotropy field B_A is about 70 T for the arsenide and 13 T for the phosphide. Thus, the magnetocrystalline anisotropy in the above compounds is almost of the same order of magnitude as that found before for other uranium pnictides, such as UCu_2P_2 [9], UAsY (Y ≡ S, Se, Te) [7, 8] and U_3X_4 (X ≡ P, As) [10].

The temperature variations in the magnetizations $\sigma_\parallel(T)$ and $\sigma_\perp(T)$ measured for $UCuP_2$ along and perpendicular to the easy c axis, respectively, are shown in figure 2. The corresponding curves for $UCuAs_2$ are presented in figure 3. The $\sigma_\parallel(T)$ and $\sigma_\perp(T)$ dependences were measured in two regimes of cooling the sample, i.e. with an applied

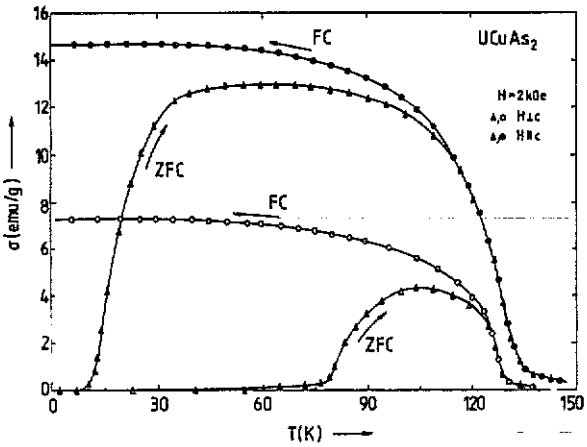

Figure 3. Magnetization versus temperature for a $UCuAs_2$ single crystal in magnetic fields parallel and perpendicular to the c axis. The FC and ZFC curves were obtained by cooling the sample with and without an applied magnetic field, respectively. Note that 1 emu $g^{-1} \equiv 0.081\mu_B$.

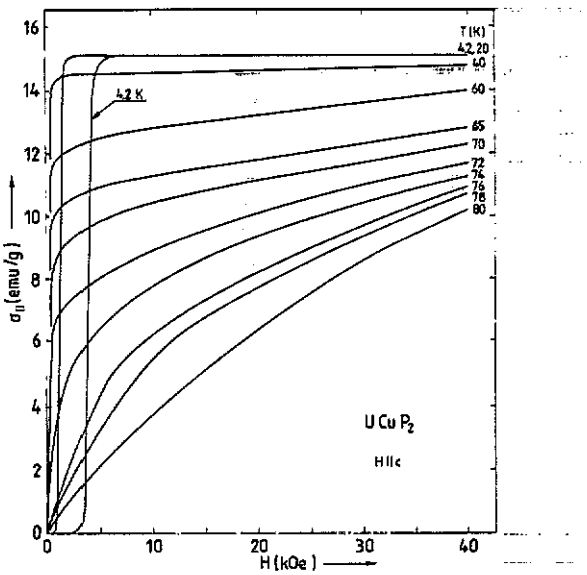

Figure 4. Magnetization versus magnetic field for a $UCuP_2$ single crystal along the easy direction at different temperatures. Note that 1 emu $g^{-1} \equiv 0.065\mu_B$.

magnetic field (field-cooled (FC)) and without (zero-field-cooled (ZFC)). The shape of these curves is typical for ferromagnets with strong domain effects [7, 8]. A characteristic broad maximum occurring in $\sigma_{\parallel}(T)$ and $\sigma_{\perp}(T)$ in the ZFC regime results from competition between the temperature-induced domain movement (leading to an increase in the sample magnetization) and the thermally driven disordering in the magnetic moment system. Such a behaviour does not appear in the $\sigma_{\parallel}(T)$ and $\sigma_{\perp}(T)$ curves in the FC regime,

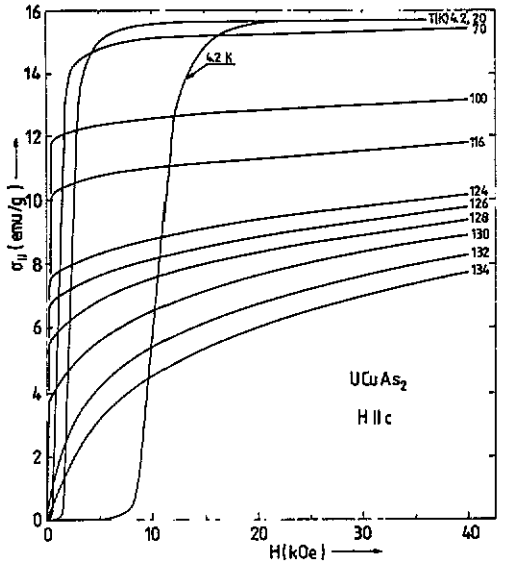

Figure 5. Magnetization versus magnetic field for a $UCuAs_2$ single crystal along the easy direction at different temperatures. Note that 1 emu $g^{-1} \equiv 0.081\mu_B$.

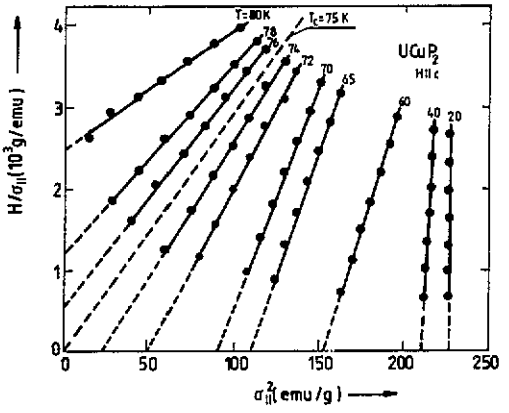

Figure 6. $H/\sigma_\parallel$ versus $\sigma_\parallel^2$ plot for a $UCuP_2$ single crystal, where $\sigma_\parallel$ is the magnetization along the easy direction.

which may correspond to the results of measurements on a single-domain crystal. The Curie temperatures of 75 K and 133 K derived in this study for $UCuP_2$ and $UCuAs_2$, respectively, agree well with those reported previously [1].

Figures 4 and 5 show the magnetization isotherms measured on $UCuP_2$ and $UCuAs_2$ single crystals oriented along the easy-magnetization axis. As seen from these figures, the $\sigma_\parallel(H)$ curves are not straight lines in some temperature regions above T_C, which results probably from the existence of a wide temperature regime of short-range magnetic interactions. The above isotherms replotted in the form of Arrott's functions, $H/\sigma_\parallel$ versus $\sigma_\parallel^2$, are straight lines for both compounds. In figure 6 we show a curve of

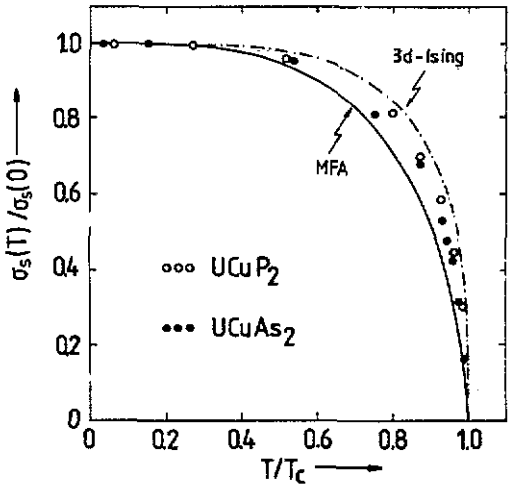

Figure 7. The reduced magnetization $\sigma(T)/\sigma_s(T)$ versus reduced temperature T/T_C for $UCuP_2$ and $UCuAs_2$ single crystals. The area of any experimental point corresponds roughly to an error made in determining the spontaneous magnetization. The full and chain curves are theoretical curves as indicated.

$H/\sigma_\parallel$ versus $\sigma_\parallel^2$ for $UCuP_2$, as an example. On the basis of such a plot, one can construct the reduced spontaneous magnetization $\sigma_s(T)/\sigma_s(0)$ versus reduced temperature (T/T_C) variations, which are displayed in figure 7 for $UCuP_2$ and $UCuAs_2$. The theoretical functions derived either from the molecular-field approximation (MFA) or from the 3D Ising model [11] are also shown. One easily sees that the experimental points of both compounds fall somewhat between these two theoretical curves, in a similar manner as found previously for UCu_2P_2 [9].

3.2. *Magnetic susceptibility*

In figure 8 are displayed the temperature variations in the inverse magnetic susceptibility for both ternary pnictides examined in this work. These $\chi_p^{-1}(T)$ functions are only slightly curvilinear and over the whole paramagnetic region studied can be well approximated by the modified Curie–Weiss law [12]

$$\chi(T) = \chi_0 + C/(T - \Theta_p). \tag{3}$$

The $\chi^{-1}(T)$ function can also be expressed as follows:

$$\chi^{-1}(T) = (A/T + B)^{-1} + \lambda \tag{4}$$

where the constant A is attributed to the paramagnetic moment μ_p of the ground state in the relation

$$\mu_p = (8A)^{1/2}(\mu_B) \tag{5}$$

the term B describes the contribution of the Van Vleck paramagnetism (enhanced in the case of metals by the Pauli susceptibility) and λ is the molecular field constant. All the parameters appearing in the above formulae were found by a least-squares fitting procedure and they are listed in table 1. From this table it is clear that the experimental

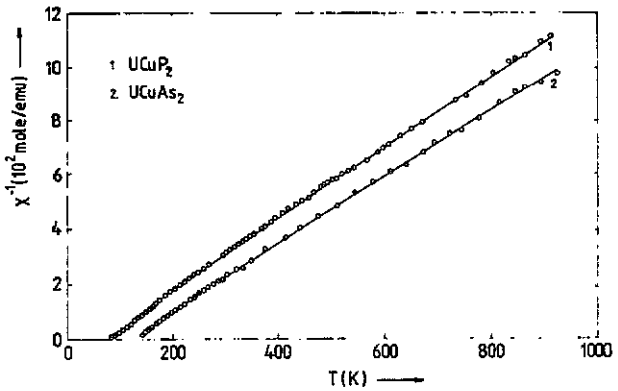

Figure 8. Thermal dependence of reciprocal molar susceptibility of $UCuP_2$ and $UCuAs_2$ powder samples up to 900 °C. Note that 100 mol $emu^{-1} \cong 12.56 \times 10^{-4}$ mol m^{-3}.

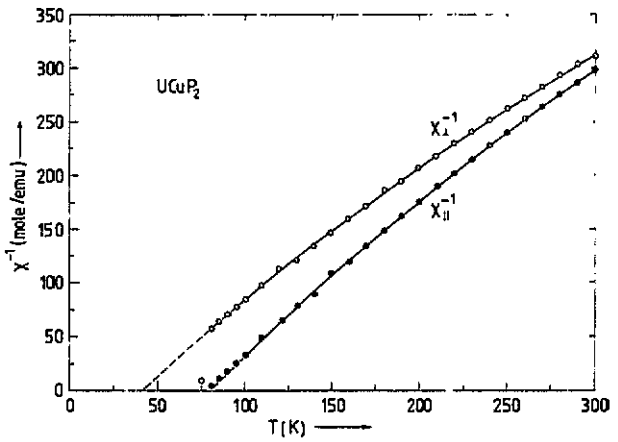

Figure 9. Thermal dependence of reciprocal molar susceptibility of $UCuP_2$ single crystal along ($\chi_{\parallel}^{-1}$) and perpendicular ($\chi_{\perp}^{-1}$) to the c axis: ———, guide for the eye. Note that 50 mol $emu^{-1} \equiv 6.28 \times 10^{-4}$ mol m^{-3}.

Table 1. Magnetic characteristics of $UCuP_2$ and $UCuAs_2$ determined on powder samples.

Compound	T_C (K)	Θ_p (K)	$10^6\chi_0$ (emu mol^{-1})	A (K emu mol^{-1})	10^6B (emu mol^{-1})	λ (emu mol^{-1})	μ_p (μ_B)
$UCuP_2$	75	70	28	0.732	28	−95	2.42
$UCuAs_2$	133	127	60	0.736	60	−166	2.46

values of the paramagnetic moment are far smaller than those expected from the $5f^2$ configuration of the U^{4+} ion or $5f^3$ configuration of the U^{3+} ion. As we have already mentioned above, this reduction mainly arises from the crystal-field interactions. Rather small values of the polarization term B usually point to a fairly large energy separation

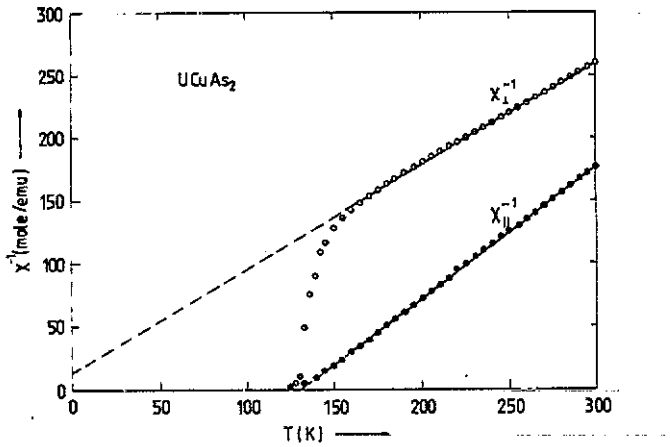

Figure 10. Thermal dependence of reciprocal molar susceptibility of $UCuAs_2$ single crystal along ($\chi_\parallel^{-1}$) and perpendicular ($\chi_\perp^{-1}$) to the c axis: ———, guide for the eye. Note that 50 mol $emu^{-1} \equiv 6.28 \times 10^{-4}$ mol m^{-3}.

Table 2. Magnetic characteristics of $UCuP_2$ and $UCuAs_2$ determined on single-crystal specimens. Values given without and in parentheses are calculated according to the CW and MCW laws, respectively.

Compound	Temperature range (K)	$\Theta_p^\parallel$ (K)	$\Theta_p^\perp$ (K)	$\chi_0^\parallel$ (10^{-4} emu mol^{-1})	$\chi_0^\perp$ (10^{-4} emu mol^{-1})
$UCuP_2$	120–300	68 (80)	30 (41)	(5.7)	(6.5)
$UCuAs_2$	160–300	131 (133)	−10 (22)	(3.0)	(9.4)

Compound	Temperature range (K)	$\mu_{eff}^\parallel$ (μ_B)	$\mu_{eff}^\perp$ (μ_B)	$\mu_s^\parallel$ (μ_B)
$UCuP_2$	120–300	2.47 (2.21)	2.62 (2.30)	0.98
$UCuAs_2$	160–300	2.77 (2.68)	3.08 (2.61)	1.27

between the ground level (or the group of closely lying energy levels) and the remaining excited crystal-field levels split by the tetragonal crystal-field potential.

The temperature dependence of the transverse and longitudinal components of the magnetic susceptibility of $UCuP_2$ and $UCuAs_2$ are shown in figures 9 and 10, respectively. As one can see, both the $\chi_\parallel^{-1}(T)$ and $\chi_\perp^{-1}(T)$ functions can roughly be approximated by the Curie–Weiss law over all the temperature interval measured. Also the fitting parameters to equation (3) are given in table 2. An apparent deviation of these curves from a straight-line behaviour when approaching the Curie temperature is caused by short-range interactions.

3.3. Electrical resistivity

The temperature dependences of the electrical resistivity of $UCuP_2$ and $UCuAs_2$, measured within the basal plane of their tetragonal unit cells ($i \perp c$), are shown in figures

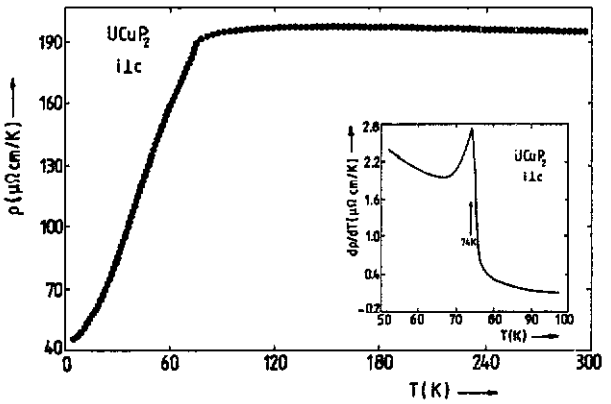

Figure 11. Thermal dependence of the electrical resistivity of $UCuP_2$ measured in the basal plane. The inset is the temperature behaviour of the derivative $d\rho_\perp/dT$ around the critical point.

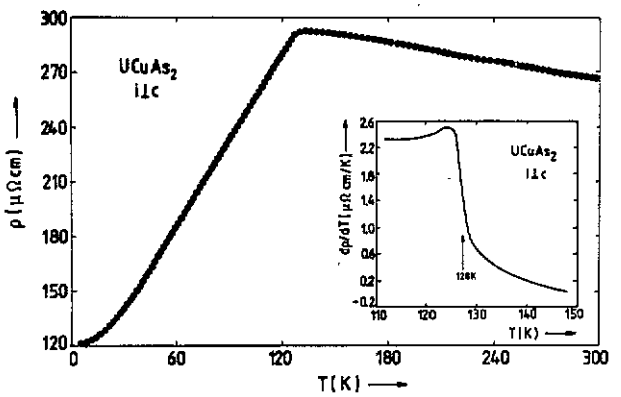

Figure 12. Thermal dependence of the electrical resistivity of $UCuAs_2$ measured in the basal plane. The inset is the temperature behaviour of the derivative $d\rho_\perp/dT$ around the critical point.

11 and 12, respectively. The shape of these curves is rather typical of many actinide ferromagnets: a strong increase in the resistivity with increasing temperature up to the critical temperature and then followed by either a slight ($UCuP_2$) or more apparent ($UCuAs_2$) tendency to decrease above this temperature. The Curie point manifests itself by a characteristic kink in $\rho(T)$, leading to a Fisher–Langer-type anomaly in the temperature derivative of the resistivity (see the insets of figures 11 and 12). The derived values of T_C for $UCuP_2$ and $UCuAs_2$, which are 74 K and 128 K, respectively, are both slightly lower than those determined in the magnetic measurements.

In the low-temperature region the resistivity for both compounds examined can be fairly well described by the equation

$$\rho(T) = \rho_0 + c_m T^2 \tag{6}$$

with the constants $\rho_0 = 48\ \mu\Omega$ cm and $c_m = 0.10\ \mu\Omega$ cm K^{-2} for $UCuP_2$ (for $T < 17$ K),

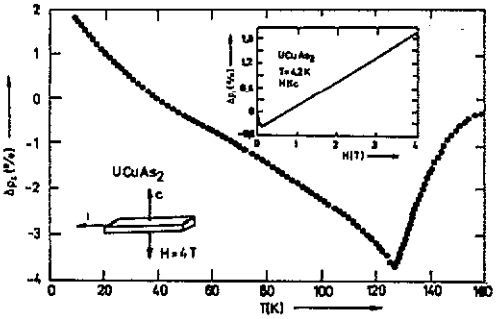

Figure 13. Magnetoresistivity $\Delta\rho_\perp$ versus temperature of $UCuAs_2$ single crystal. The upper right inset shows the magnetoresistivity $\Delta\rho_\perp$ at 4.2 K as a function of magnetic field oriented parallel to the c axis. The lower left inset gives the direction of the current and applied magnetic field in relation to the c axis of a crystal.

and $\rho_0 = 120\ \mu\Omega$ cm and $c_m = 0.02\ \mu\Omega$ cm K^{-2} for $UCuAs_2$ (for $T < 45$ K). Assuming the validity of the Matthiessen rule, ρ_0 in equation (6) is the residual resistivity while the second term describes scattering processes of the electron–magnon type.

The observed behaviour of $\rho(T)$ for these two ternary pnictides in the paramagnetic region suggests the presence of a Kondo-like effect. However, because of the limited temperature range of our measurements ($T < 300$ K) we could not perform any reliable analysis of $\rho(T)$. Fortunately, in the meantime one of us (DK) undertook electrical resistivity measurements of $UCuP_2$ and $UCuAs_2$ up to 1000 K at Eidgenössiche Technische Hochschule Zürich and hence an extensive discussion of the transport properties of these two compounds was possible [13, 14]. It has been shown that indeed the resistivity for both ternary pnictides follows the standard Kondo formula over a wide temperature range.

3.4. Magnetoresistivity

Figure 13 presents the transverse magnetoresistivity ($\boldsymbol{i} \perp \boldsymbol{H}$) of $UCuAs_2$ taken along the easy-magnetization axis ($\boldsymbol{H} \| \boldsymbol{c}$) at a field of 4 T. It appears from this figure that the magnetoresistivity of $UCuAs_2$ is mostly negative and the $\Delta\rho_\perp(T)$ curve reveals a sharp minimum at the Curie temperature. Such a behaviour is characteristic of uniaxial ferromagnets, as predicted theoretically by Yamada and Takada [15] and for example proved experimentally in studies of UAsSe [16]. However, in the low-temperature region (below 37 K) the magnetoresistivity of $UCuAs_2$ at 4 T becomes positive. The field dependence of $\Delta\rho_\perp$ measured at 4.2 K is displayed in the inset to figure 13. The magnetoresistivity of $UCuAs_2$ in low magnetic fields first rises negatively, then goes through a minimum at about 0.1 T and finally increases linearly up to 2% at 4 T.

In contrast with $UCuAs_2$, the transverse magnetoresistivity of $UCuP_2$ measured at 4.2 K is almost independent of the applied magnetic field and its value is lower than 0.1%.

4. Discussion

The crystal structures of $UCuP_2$ [6] and $UCuAs_2$ [3] are both very close to that of their parent compounds, i.e. UP_2 and UAs_2 [17]. The difference is that the unit cells of the

former compounds contain additionally the planes of the Cu atoms which increase their c/a-ratio by about 17% compared with those of their homologues. It is interesting to note that this insertion of the Cu atom planes into the $UCuP_2$ and $UCuAs_2$ unit cells leads to a change in the magnetic order from the antiferromagnetic to ferromagnetic with a simultaneous decrease in the ordering temperature to more than half [17]. In contrast, such planes but containing Ni or Pd atoms leave the same magnetic arrangement and the Néel temperature drops by only about 18% or 15%, respectively [1, 5].

Despite the differences between the crystal structures of $UCuP_2$ and $UCuAs_2$, in both cases the uranium atoms occupy the position of C_{4v} symmetry. The corresponding Hamiltonian

$$H_{CEF} = B_2^0\hat{O}_2^0 + B_4^0\hat{O}_4^0 + B_4^4\hat{O}_4^4 + B_6^0\hat{O}_6^0 + B_6^4\hat{O}_6^4 \tag{7}$$

where B_n^m and $\hat{O}_n^m$ are the crystal-electrical-field (CEF) parameters and Stevens equivalent operators, respectively, splits the ground multiplet $^3H_4$ of U^{4+} into seven crystal-field levels: two doublets $\Gamma_{5t}^{(1,2)}$ with the wavefunctions containing the $|\pm 3\rangle$ and $|\mp 1\rangle$ states (equation (8)), three singlets $\Gamma_{1t}^{(1,2)}$ and Γ_{2t} comprising the $|4\rangle$, $|0\rangle$ and $|-4\rangle$ states and two singlets Γ_{3t} and Γ_{4t} built up of the $|2\rangle$ and $|-2\rangle$ states.

The crystal-field potential relevant to the C_{4v} point group has previously been described in detail [18]. In [18] it was shown that a Γ_{5t} doublet (potentially being for most tetragonal uranium compounds a ground state), for which the wavefunction takes the form

$$|\Gamma_{5t}\rangle = \cos\alpha\,|\pm 3\rangle \pm \sin\alpha\,|\mp 1\rangle \tag{8}$$

has a strong uniaxial character. This arises from the fact that the magnetic susceptibility component $\chi_\perp$ perpendicular to the c axis is zero. This also implies that μ_p and μ_s at temperatures close to 0 K should have the same magnitudes, as for example was the case of the tetragonal uranium compounds U_2N_2Sb and U_2N_2Bi [18].

In our case both the effective magnetic moments $\mu_{eff}^{\parallel}$ and $\mu_{eff}^{\perp}$ (table 2), but especially the values μ_p given in table 1 which were determined at 0 K on the basis of equations (4) and (5), are relatively large and considerably exceed the relevant magnitudes of μ_s. Because of insufficient numbers of experimental data and a rather small temperature range for our single-crystal measurements, it was not possible to fit to the experimental susceptibility curves $\chi_\parallel(T)$ and $\chi_\perp(T)$ any known phenomenological CEF model (see, e.g., [19–21]). However, on the basis of the observed tendency to follow the Curie–Weiss law by both components of the susceptibility, it seems that the ground state of $UCuP_2$ as well as of $UCuAs_2$ consists of several closely lying CEF levels (being well populated in the temperature region of the ordered state), while the remaining levels are energetically pushed away from such a 'ground state'. Moreover a Γ_{5f} doublet certainly plays the fundamental role in the ground-state properties of these compounds because of the observed strong confinement of the ordered moment to the c axis.

A comparison of the magnitudes of the critical field B_{nf}, the anisotropy constant K_1 and the difference $(\chi_\parallel - \chi_\perp)$ between the susceptibilities at a given temperature for $UCuP_2$ and $UCuAs_2$ gives evidence of the larger magnetocrystalline anisotropy present in the latter compound, although from the point of view of CEF interactions one could expect the reverse situation, because of the larger distances between the central ion and ligands in the arsenide. This situation has to cause a decrease in the magnitude of the CEF potential and thereby reduce the total magnetocrystalline anisotropy. Therefore the observed difference between the magnetic behaviours and crystal structures of these two pnictides probably arises from the covalency effect, which is more pronounced in

the phosphide. Also an increase in f localization in the sequence $UCuP_2$, $UCuAs_2$ and UCu_2P_2 has been found in the optical and magneto-optical studies of these compounds [22, 23]. The latter conclusion is also consistent with the observed increase in the ordered moment and the ordering temperature on going along the sequence of compounds mentioned above.

5. Conclusions

We have made detailed susceptibility, magnetization and electrical measurements on single-crystal samples of $UCuP_2$ and $UCuAs_2$. These compounds were found to exhibit fairly large values of the anisotropy field B_A, which are 13 T and 70 T, respectively. These values can be compared with $B_A \simeq 100$ T, found for mostly anisotropic material in this series of ternary compounds, UCu_2P_2 [9]. All these data strongly reflect the local picture of the magnetism in these ternary compounds and hence the important role of crystal-field interactions. This single-ion anisotropy, however, should be modified by the presence, especially in the 1:1:2-type ternary pnictides, of Kondo and covalency effects. On the other hand, the hybridization(exchange)-induced anisotropy in such a type of compounds is very often regarded as predominant. Therefore, it seems that all these three ternary pnictides are good candidates for more detailed studies to determine the respective mechanism in the observed anisotropy.

References

[1] Zołnierek Z, Kaczorowski D, Troć R and Noël H 1986 *J. Less-Common Met.* **121** 193
[2] Kaczorowski D 1989 *Abstracts 19èmes Journees des Actinides (Madonna di Campiglio, 1989)* p 55
[3] Stepień-Damm J, Kaczorowski D and Troć R 1987 *J. Less-Common Met.* **132** 15
[4] Fischer P, Murasik A, Kaczorowski D and Troć R 1989 *Physica* B **156–7** 829
[5] Murasik A, Fischer P and Kaczorowski D 1990 *J. Phys.: Condens. Matter* 2 3967
[6] Noël H, Zołnierek Z, Kaczorowski D and Troć R 1987 *J. Less-Common Met.* **132** 327
[7] Bazan C and Zygmunt A 1972 *Phys. Status Solidi* **12** 649
[8] Bielov K P, Dmitrievskii A S, Zygmunt A, Levitin R Z and Trzebiatowski W 1973 *Zh. Eksp. Teor. Fiz.* **64** 582
[9] Kaczorowski D and Troć R 1990 *J. Phys.: Condens. Matter* 2 4185
[10] Zeleny M 1981 *Czech. J. Phys.* B **31** 309 and references therein
[11] Guttman A J, Domb C and Fox P E 1971 *J. Physique* **32** 354
[12] Amoretti G and Fournier J M 1984 *J. Magn. Magn. Mater.* **43** L217
[13] Korner N, Schoenes J and Kaczorowski D 1989 *Helv. Phys. Acta* **62** 207
[14] Kaczorowski D and Schoenes J 1990 *Solid State Commun.* **74** 143
[15] Yamada H and Takada S 1973 *J. Phys. Soc. Japan* **34** 51
[16] Wojakowski A and Henkie Z 1977 *Acta Phys. Pol.* A **52** 401
[17] Troć R 1987 *Inorg. Chim. Acta* **140** 67
[18] Zołnierek Z and Troć R 1978 *J. Magn. Magn. Mater.* **8** 210
[19] Amoretti G, Blaise A and Mulak J 1984 *J. Magn. Magn. Mater.* **42** 65
[20] Nieuwenhuys G J 1987 *Phys. Rev.* B **35** 5260
[21] Kaczorowski D 1987 *J. Magn. Magn. Mater.* **76–7** 366
[22] Schoenes J, Fumagalli P, Rüegsegger H and Kaczorowski D 1989 *J. Magn. Magn. Mater.* **81** 112
[23] Fumagalli P, Schoenes J and Kaczorowski D 1988 *Solid State Commun.* **65** 173